

IN SEARCH OF THE MATERIAL COMPOSITION OF REFUSE-DERIVED FUELS BY MEANS OF DATA RECONCILIATION AND GRAPHICAL REPRESENTATION

Therese Schwarzboeck, Manuel Hahn *, Stefan Spacek and Johann Fellner

Institute for Water Quality and Resource Management, TU Wien, Karlsplatz 13/226-02, 1040 Vienna, Austria

Article Info:

Received:
25 July 2022
Revised:
20 February 2023
Accepted:
15 March 2023
Available online:
31 March 2023

Keywords:

Refuse-derived fuels
Biomass content
Balance equations
Elemental composition
Non-linear data reconciliation
Probability density egg


ABSTRACT

Differentiating between material fractions in refuse-derived fuels (RDF) is relevant to determining the climate relevance of RDF (fractions of biomass and fossil matter). This differentiation is associated with analytical challenges. A method was applied using balance equations, which contain the elemental composition (C, H, N, S, O) of the RDF and the sought for material fractions. For the first time this so-called adapted Balance Method (aBM) was applied to oil-contaminated RDF with the aim of not only distinguishing between biomass and fossil matter but between fossil matter from plastics and from oil-contamination as well. Thus, the balance equations and the following data reconciliation was adapted. It is shown that the balance method is based on mathematics that provides valuable insight far beyond the basic types of calculation since the calculation takes place in higher dimensions. It is also shown that the operation of the algorithm can be represented graphically in the lower third dimension. The mass of oil contamination as well as the mass of biogenic and fossil matter could be determined for the RDF considered. Problems concerning relatively high uncertainties still need to be solved due to the similar elemental composition of plastics and oil. However, it is shown that the aBM is capable of distinguishing between more than two material fractions in RDF, which the other available methods cannot and which can be relevant for greenhouse gas reporting but also for process control purposes.

1. INTRODUCTION

In the course of the shift from landfilling to thermal recovery of waste in recent decades, the amount of greenhouse gases from the sector of waste management has significantly declined (e.g. reduction by 72% from 1990 to 2021 in Austria; Anderl et al. 2023). Substituting fossil fuels in industrial plants with refuse-derived fuels (RDF) can lower costs for primary raw materials and can also reduce emissions of climate-relevant CO₂ (e.g. Aranda Usón et al., 2013, Garg et al., 2007, Genon & Brizio, 2008, Habert et al. 2010). However, individual RDF contain both climate-neutral biomass and significant amounts of materials of fossil origin (plastics) (e.g. Hiromi Ariyaratne et al. 2014, Nasrullah et al, 2015, Sarc et al, 2014). Thus, in order to determine the amount of reduced climate-relevant CO₂, it is necessary to differentiate between the material fractions of biomass and fossil materials. When utilizing RDF in waste-to-energy plants or in industrial plants, such as cement works, only CO₂ of fossil origin is accounted for as climate relevant and therefore defines the actually mitigated CO₂ emissions

(European Parliament, 2009). In practice, differentiating between biomass and fossil matter in the feedstock is associated with analytical challenges (Fellner & Rechberger, 2009, Hiromi Ariyaratne et al., 2014, Larsen et al., 2013, Moora et al., 2017, Muir et al., 2015, Schwarzböck et al., 2018a). Three methods are described in Standard EN ISO 21644: Manual Sorting (MS), Selective Dissolution Method (SDM), and Radiocarbon Method (14C-method). MS cannot be applied as a stand-alone method; another method has to be used to determine the biomass share in unknown material fractions (e.g. composites, textiles, fine fraction). SDM has some unknown uncertainties as some fossil materials are unintentionally chemically dissolved (e.g. some types of textiles, polyurethane) and are thereby wrongly categorized as biomass. 14C-method is connected with high analytical efforts and high costs. A further method has been developed and validated in recent years - the adapted Balance Method (aBM) (Fellner et al. 2011, Schwarzböck, 2018, Schwarzböck et al., 2018a, Schwarzboeck et al., 2018b). The aBM makes use of significant differences between the elemental composition (C, H, N, S, O) of fossil and biogenic

 * Corresponding author:
Manuel Hahn
email: manuel.hahn@tuwien.ac.at

materials. Balance equations are set up for each element, the elemental composition in the RDF is analytically determined and, by means of a mathematical solution, the fossil and biogenic material fractions can be derived.

The scope of application for all methods mentioned is currently solid recovered fuels, which are RDF derived from non-hazardous waste and comply with the European Standard (EN ISO 21640). Moreover, all of the methods envisage differentiation into two material fractions in SRF (biogenic, fossil). However, also for RDF derived from hazardous waste determining the climate relevance might be of interest. Further, more information can be relevant regarding the materials contained in RDF (e.g. different types of plastics, contaminations in RDF, share of food waste) (Galcko et al., 2023, Rada & Ragazzi, 2014, Viczek et al., 2020). As the aBM-methodology works with a mathematical solution (non-linear data-reconciliation), it has the potential to ensure that further information be easily extractable when the algorithm is adapted.

Thus, the study presented works on further advancing the aBM-methodology. For the first time, RDF which are contaminated with waste oil are investigated regarding their fossil and biogenic fraction.

The objectives of the study are:

- to generate input parameters for applying the aBM for this specific type of RDF (elemental composition of the biogenic and fossil fraction and of the oil contained in the RDF)

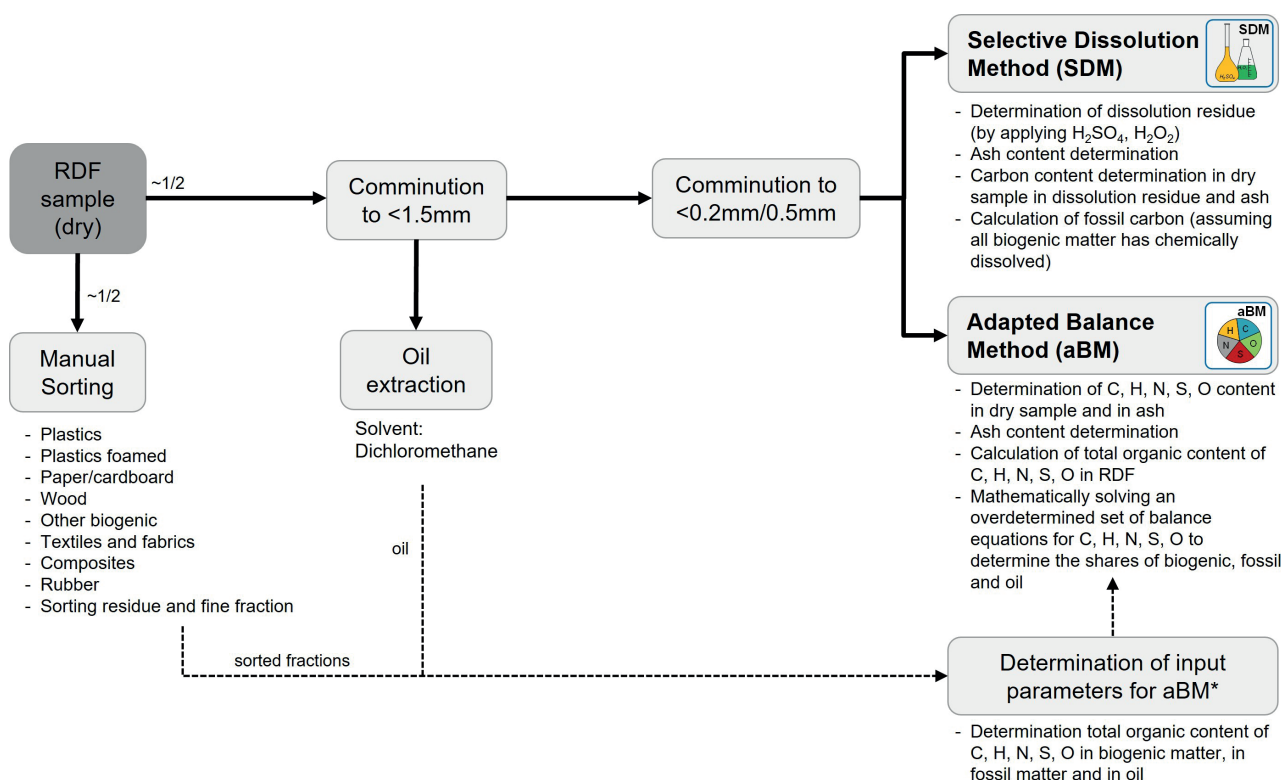
- to adapt the balance equations so that three mass shares in the RDF can be determined (biogenic, fossil, oil) by using only elemental analyses and balance equations (aBM)
- to introduce a graphical representation of the mathematical pathway (normal distribution in the 3rd dimension, and the graphical description of the expected value and variance in the 3rd dimension), and
- to introduce a graphical representation of the algorithm of the non-linear data reconciliation in the 3rd dimension.

Some papers have been published presenting a graphical representation of similar mathematical solutions, but most of them are limited to two-dimensional distributions and only a few also graphically consider a 3-dimensional normal distribution. (Rueda & Oommen, 2003).

2. METHODS

2.1 Oil-contaminated refuse-derived fuel samples and sample preparation

RDF samples which are contaminated with petroleum waste oil were investigated (particle size <50mm). 10 composite samples (each ~3 kg) were drawn from an RDF production plant over a period of one week (note: results for only one sample are shown as the focus of the work is dedicated to the mathematical solution required by the aBM).



* Input parameters have to be determined only once for each RDF. For further samples, this step is not necessary any more (also literature values or data already collected could be used, e.g. Schwarzboeck et al., 2018b)

FIGURE 1: Sample preparation procedure and methods applied for oil-contaminated RDF.

Sample preparations steps conducted for the present study are shown in Figure 1. Half of each sample was used to generate a "sorting sample".

The waste oil was extracted in order to also determine the elemental composition of the contained oil (used as input-parameter for aBM). The oil extraction was conducted by using a Soxhlett apparatus and by using the solvent Dichloromethane at a temperature of over 40°C.

2.1.1 Sorting

Samples were sorted into 9 fractions (see Figure 1). This is to generate input-parameters for the aBM (water- and ash-free elemental composition of fossil matter and of biogenic matter).

These input parameters only need to be determined once for each RDF stream and could also be derived from literature values if the general composition of the RDF (e.g. major sources of biogenic and fossil matter present in the RDF, such as paper, PE, PP) is known. In this case, RDF-specific values were generated as this RDF represents a new type of RDF investigated. Already collected data on aBM input parameters for the aBM can be found in Schwarzboeck et al., 2018b.

2.1.2 Sample comminution

The samples were comminuted down to a grain size of below 0.2 mm (plastics below 0.5 mm). A cutting mill (Retsch SM 2000) and an ultracentrifugal mill (Retsch ZM 200) were applied (with liquid nitrogen for cooling) to produce analysis samples. A riffle divider and rotary divider were used to reduce the sample mass between the grinding steps.

2.2 Analyses

2.2.1 Elemental analyses for aBM

CHNSO elemental analysis (C - Carbon, H - Hydrogen, N - Nitrogen, S - Sulphur, O - Oxygen) was applied to determine the water-and-ash-free elemental composition of the RDF samples. This is necessary in order to apply the aBM. Elemental analyses were also applied to the sorted fractions in order to define the elemental composition of water- and ash-free biogenic and fossil matter (see details in section 2.3.5.).

The water-free analysis samples were analysed by means of an Vario Macro instrument (for CHNS-analysis) and a Rapid OxyCube (for O-analysis, based on pyrolysis) (both instruments from Elementar Analysensysteme GmbH, Hanau, Germany). At a combustion temperature of 1,150 °C (pyrolysis temperature of 1,450°C for O), the total carbon (TC), total hydrogen (TH), total nitrogen (TN), total sulphur (TS) and total oxygen (TO) content is determined according to EN 15407:2011. Each sample is analyzed at least 3-fold (for O at least 5-fold), with each measurement comprising 30 to 40 mg (for O 6 to 10 mg), depending on the material. Additionally, the ash content of each analysis sample is determined according to EN 15403:2011 and analysed for the inorganic content of C, H, N, S and O. Elemental analyses of ash were done 2-fold with 55 to 60 mg (for O 4 to 10 mg).

The extracted oil was also analysed for its CHNSO composition following the same analytical procedure.

2.2.2 Selective Dissolution Method (SDM)

The Selective Dissolution Method was applied to oil-extracted samples according to EN ISO 21644. Two batches for each sample were analysed by SDM using 5 g of sample each (grain size below 0.5 mm) and applying sulphuric acid (78%) and hydrogen peroxide (30%). This should dissolve the biogenic matter contained in the sample. After 16 h the process was stopped and the samples were filtered, rinsed and dried. The dissolution residue (assumably containing only fossil and inert materials) was analysed for its carbon content and ash content in order to determine the fossil and biogenic carbon content in the sample (see EN ISO 21644 for calculation procedure).

2.3 Adapted Balance Method (aBM) to determine three mass shares

The adapted Balance Method relies on the different elemental composition of the material fractions contained in the RDF sample. In this case the assumption is that the fractions of biogenic matter, fossil matter (plastics) and waste oil (also fossil) have different elemental compositions (on a water- and ash-free basis).

Balance equations are set up for each element (carbon, hydrogen, oxygen, nitrogen and sulphur). Each contains the (unknown) mass shares of the target fractions. Thus, an overdetermined set of equations has to be solved. Thereto a mathematical balancing algorithm is used and the mass shares of the three target fractions are derived. The following four sections explain how this optimization problem is solved.

2.3.1 Balance equations and variable vector, non-information-carrying variables

Ω is the variable vector in the n^{th} dimensional Space ($n=26$). Thus, 26 variables are defined:

$$\Omega = (m_i, TC_{RDF}, TH_{RDF}, TO_{RDF}, TN_{RDF}, TS_{RDF}, TC_i, TH_i, TO_i, TN_i, TS_i, C_{Cb}, C_{Hb}, C_{Ob}, C_{Nb}, C_{Sb}, C_{Cb}, C_{Hf}, C_{Of}, C_{Nf}, C_{Sf}, C_{Cp}, C_{Hp}, C_{Op}, C_{Np}, C_{Sp})$$

Where indices refer to:

- C** Carbon
- H** Hydrogen
- O** Oxygen
- N** Nitrogen
- S** Sulphur
- i* inert matter
- C* concentration
- b* biogenic
- f* fossil
- p* petroleum (oil)
- RDF* refuse derived fuel

Thus, variables refer to:

m_i inert matter contained in the water-free RDF [kg/kg_{wf}]

$TC_{RDF}, TH_{RDF}, TO_{RDF}, TN_{RDF}, TS_{RDF}$
total content of carbon, hydrogen, oxygen, nitrogen, and sulphur in the water-free RDF [g/kg_{wf}]; determined by laboratory analyses of the RDF

$TC_i, TH_i, TO_i, TN_i, TS_i$

total content of carbon, hydrogen, oxygen, nitrogen, and sulphur in the ash of the RDF [g/kg_{ash}]; determined by laboratory analyses

$C_{Cb}, C_{Hb}, C_{Ob}, C_{Nb}, C_{Sb}$

water- and ash-free elemental composition of biogenic matter [g/kg_{waf}]; determined by sorting and analyses (one-time) or by using literature values

$C_{Cf}, C_{Hf}, C_{Of}, C_{Nf}, C_{Sf}$

water- and ash-free elemental composition of fossil matter [g/kg_{waf}]; determined by sorting and analyses (one-time) or by using literature values

$C_{Cp}, C_{Hp}, C_{Op}, C_{Np}, C_{Sp}$

water- and ash-free composition of (petrochemical) oil contained in the RDF [g/kg_{waf}]; determined by analyses (one-time) or by using literature values

m ($m=6$) is the number of non-linear equations (constraints). The following equations are defined:

$$f_1(\Omega) = m_b + m_f + m_i + m_p - 1 = 0$$

$$f_2(\Omega) = m_b * C_{Cb} + m_f * C_{Cf} + m_p * C_{Cp} + m_i * TC_i - TC_{RDF} = 0$$

$$f_3(\Omega) = m_b * C_{Hb} + m_f * C_{Hf} + m_p * C_{Hp} + m_i * TH_i - TH_{RDF} = 0$$

$$f_4(\Omega) = m_b * C_{Ob} + m_f * C_{Of} + m_p * C_{Op} + m_i * TO_i - TO_{RDF} = 0$$

$$f_5(\Omega) = m_b * C_{Nb} + m_f * C_{Nf} + m_p * C_{Np} + m_i * TN_i - TN_{RDF} = 0$$

$$f_6(\Omega) = m_b * C_{Sb} + m_f * C_{Sf} + m_p * C_{Sp} + m_i * TS_i - TS_{RDF} = 0$$

Where,

f_1 Mass Balance

f_2 Carbon Balance

f_3 Hydrogen Balance

f_4 Oxygen Balance

f_5 Nitrogen Balance

f_6 Sulphur Balance

l ($l=3$) is the number of non-information-carrying (unknown) variables. The three variables m_b, m_f, m_p are to be calculated.

Where,

m_b biogenic matter contained in the water-free RDF [kg/kg_{wf}]

m_f fossil matter contained in the water-free RDF [kg/kg_{wf}]

m_p matter of waste oil (index p petroleum) contained in the water-free RDF [kg/kg_{wf}]

m_i inert matter contained in the water-free RDF [kg/kg_{wf}]

In addition, the whole system is connected to a mathematical restriction that is defined with the following inequality:

$$l \leq m \leq n$$

Where,

n number of variables

m number of non-linear equations

l number of non-information-carrying (unknown) variables

2.3.2 Mathematical background in the n^{th} dimension

First we define an n -dimensional variable vector Ω with all variables. Over this n -dimensional domain we define a

scalar field that represents a probability density of an n -dimensional normal distribution. This scalar field is equal to the square of the Mahalanobis distance in the n^{th} dimension. The next step is to define a set of m non-linear equations. This set represents m constraints in n -dimensional space. The goal is to find an extremum (point with the largest probability density) of the n -dimensional probability density, but not in the entire n -dimensional space since not all points in the entire n -dimensional space fulfill all constraint conditions. The number of m equations defines a $(n-m)$ -dimensional manifold, which is a subset of the entire n -dimensional space. It follows that all points of the variable vector Ω from the $(n-m)$ -dimensional manifold are a solution to the non-linear system of equations.

Within the next step, using the Lagrange multiplier method, $(m+n)$ non-linear equations with m additional variables (Lagrange multipliers) are derived. This changes the system of equations from being overdetermined to a system of equations that guarantees a solution. But the problem is that you would have to solve a non-linear system of equations with $(m+n)$ equations and $(m+n)$ variables. Therefore, the equations are linearized locally by means of a Taylor series ending after the linear term. This means that this step has to be repeated iteratively several times until the maximum of the normal distribution restricted to the set of manifolds is found. Mathematically, the following happens specifically in each step of the iteration: the maximum of the scalar field on the manifold is not sought directly, but from a numerical scalar field on the respective mapping of the manifold. The respective mapping is a $(m-n)$ -dimensional vector space. If the m equations contain unknown variables in addition to the known variables, the system of equations must be cleaned of these non-information-carrying variables. This is done using the Gaussian elimination method. After the maximum of the variables has been found, the non-information-carrying (unknown) variables are calculated from these variables.

In the case of a linear constraint, the calculation is greatly simplified. The solution is calculated directly on the intersection of the linear constraint (linear vector space) with the probability density in just one calculation step instead of several iterative steps (Wu et al., 2016).

In summary, in order to understand the precise mathematical process, the theory of the Lagrange multiplier and the theory of manifolds are required as background knowledge. Therefore, section 2.3.4 gives an overview of how to graphically display all the calculation steps for a 3-dimensional normal distribution.

2.3.3 Mathematical background in the 3rd dimension

The graphical interpretation of the 3-dimensional normal distribution can be understood by comparing it with the 1-dimensional normal distribution (shown in Figure 2). For the graphic analysis, the formula of the 1-dimensional normal distribution density can be reduced to the following simple form:

$$h(x) = x^2 \text{ parabola}$$

$$g(x) = -x^2 \text{ negative parabola (reflection around the x-axis)}$$

$$f(x) = f(g(x)) = e^{-x^2} \text{ density of the normal distribution without}$$

normalization factor
 x normally distributed random variable

The following important finding can be derived from the analysis of Figure 2: At the same point ($x=0$) where the parabola has its minimum, the density of the normal distribution has a maximum. It follows that in order to calculate the maximum of the normal distribution, one has to find the minimum of the parabola. The reason is that the exponential function has only the following two effects on the negative parabola function: i) The parabola is compressed along the 1st dimension, ii) A translation is performed along the 2nd dimension:

$$g(x=0) = 0 \rightarrow f(x=0) = 1$$

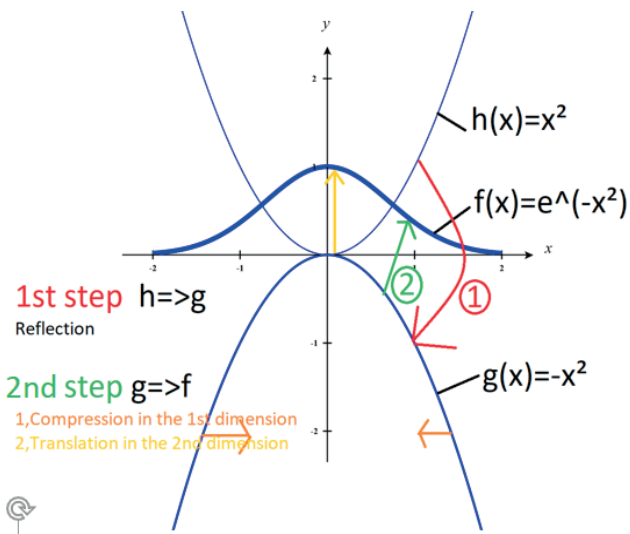


FIGURE 2: Graphical interpretation of a 1-dimensional normal distribution.

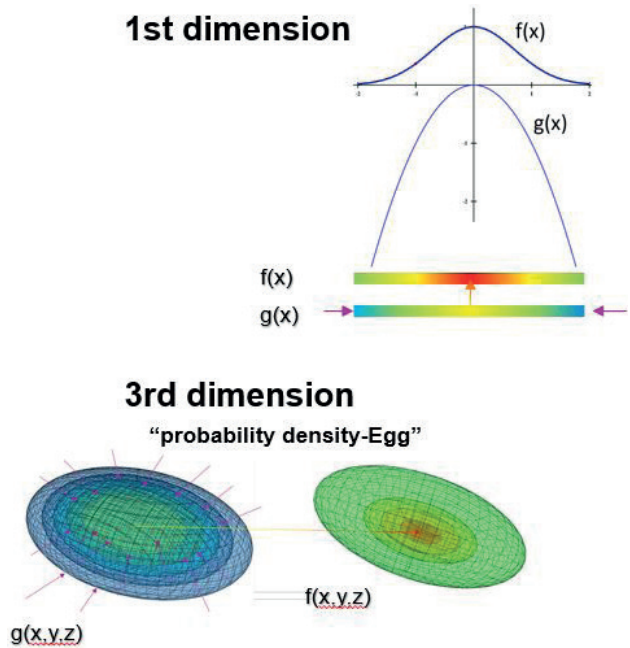


FIGURE 3: Comparison of 1-dimensional to a 3-dimensional normal distribution.

Figure 3 shows that the transformation from the parabola to the bell curve can be shown in a 2-dimensional graphic. However, this has the disadvantage that you would need the 4th dimension for this type of graphic for the 3-dimensional normal distribution density. But you can also represent the whole transformation in just a one-dimensional graphic. In this, the level of the probability density is represented by the color. Red represents a high probability and blue represents a low probability.

Before we interpret the density of the 3-dimensional normal distribution graphically, the effect of the parameters μ, σ^2 in the formula is discussed:

$$f(x) = e^{-\frac{(x-\mu)^2}{\sigma^2}}$$

μ expected value
 σ^2 variance

The expected value μ is simply a translation of the maximum of the density of the normal distribution from the position $x=0$ to the position $x=\mu$ (the effect of the whole bell curve being shifted by μ in the positive x direction). The variance σ^2 only leads to a greater width of the bell (the additional normalization factor would also reduce the height of the bell).

Now the density of the 3-dimensional normal distribution will be discussed, the graphical representation of which will henceforth be called the "probability density egg" (reason for this name is given below).

$$h(x, y, z) = \frac{(x-\mu_x)^2}{\sigma_x^2} + \frac{(y-\mu_y)^2}{\sigma_y^2} + \frac{(z-\mu_z)^2}{\sigma_z^2} := r(x, y, z)^2$$

$$f(x, y, z) = f(h(x, y, z)) = e^{-\frac{(x-\mu_x)^2}{\sigma_x^2} + \frac{(y-\mu_y)^2}{\sigma_y^2} + \frac{(z-\mu_z)^2}{\sigma_z^2}}$$

x, y, z three normally distributed random variables
 $(\mu_x, \mu_y, \mu_z) := \mu$ vector of expected value (defines the position of the maximum of the probability density egg)
 r Mahalanobis distance (Ke et al., 2018)

$$\begin{pmatrix} \sigma_x^2 & 0 & 0 \\ 0 & \sigma_y^2 & 0 \\ 0 & 0 & \sigma_z^2 \end{pmatrix} := V$$

V Covariance matrix

For all positions (x, y, z) where $r = \text{const}$, $h(x, y, z) = \text{const}$ is the implicit equation of an ellipsoid. The center of this ellipsoid in 3-dimensional space is defined by the vector μ ; and the shape of the ellipsoid is defined by the variance of x, y, z . When the special case $\sigma_x^2 = \sigma_y^2 = \sigma_z^2 \dots$ occurs, the ellipsoid becomes a spherical surface. From this follows the difference between the variances of x, y, z , graphically represented by the deviation of the sphere's surface in the respective direction. The variable (x, y, z) with the greatest variance deviates the most from the sphere (the sphere is bent the most into an egg) and the variable with the smallest variance deviates less from the sphere (so a variance with ≈ 1 describes a spherical surface in this direction).

Figure 3 shows five layers of this ellipsoid (each of the layers is defined by a different r value). Instead of these individual layers, you have to imagine closely packed layers (for all positive real numbers (r)). The exponential function

of these ellipsoids is then a compression in the 3rd dimension and a translation through the 4th dimension. This leads to the fact that the simple ellipsoid becomes a probability density function $f(x,y,z)$, similar to a mass density of an object). The most important thing can be seen from the graphic (Figure 3): The simple ellipsoid has its center at the same position in the 3-dimensional space where the probability density function has its maximum (position= μ at the expectation value). This is the reason why the 3-dimensional probability density function is named "probability density egg" (Figure 4).

Note that it was assumed that the variables x,y,z are statistically independent (all values (covariances) in the covariance matrix that are not on the main diagonal are zero). If there is a correlation between the variables x,y,z (if covariances exist), it is possible to describe the probability density in a new coordinate system (coordinate transformation $(x,y,z) \rightarrow (u,v,w)$) in which the variables (u,v,w) are again statistically independent (covariances disappear). Note that there always exists a coordinate system for each covariance matrix. The topic of covariances and details thereon, however, would go beyond the scope of this paper (in the literature this mathematical theory can be found under the name "Principal axis theorem").

2.3.4 Graphical representation of data reconciliation in the 3rd dimension

Here it was described how to graphically represent a 3-dimensional normal distribution (probability density egg). The most important thing repeated: the expected value vector defines the position of the value with the highest probability density, and the covariance matrix defines in which variable direction the egg deviates the most from a spherical surface. From the estimator theory ("Maximum likelihood estimation") it follows that the arithmetic mean of the values measured is an unbiased estimator for the expected value and the sample variance estimates the expected variance.

$$m(x,y,z)=a*x+b*y+c*z-d=0$$

a,b,c,d constant coefficients

In the simplest case, the linear regression calculation has an additional constraint defined by a balance equation ($m(x,y,z)$) which must be fulfilled (but there can also be several equations). But if you put the measured values of x,y,z (the unbiased estimates for the expected value) into this equation, you can see that they do not satisfy the equation. Graphically, an equation defines a plane in 3-dimensional space - in the space in which the probability density egg resides (see Figure 5). The solution to the least squares equation is on the intersection of the egg with this plane (more precisely the point on this plane with the highest probability density). In summary, in linear data reconciliation one simply searches for the position of the maximum of the probability density, but instead of searching in the whole space, the search is restricted to the level defined by the constraint.

$$q(x,y,z)=x^2+y^2+z^2-25=0$$

The graphic representation for finding the solution to the non-linear regression calculation is shown in Figure 6. In this case the constraint describes a curved surface in space (manifold) instead of a plane. As an example, Figure 6 shows a spherical surface $q(x,y,z)$ (radius 5) which again intersects the layers of the probability density egg. However, one does not look for the solution on the cut surface (part of the spherical surface) in a non-linear step, but takes the detour over several small steps (iterative approximation). More precisely, one creates linear maps of the manifold by linearizing the constraint. The exact description cannot be discussed here as it would drift too far into higher mathematics. One can simply think of it as follows (see Figure 6): The starting position is defined by the mean vector. From there you look at the surface of the sphere and perceive it as a disc. However, this disc that you see does not touch the sphere's surface but hovers in space between the sphere's surface and the starting position. This

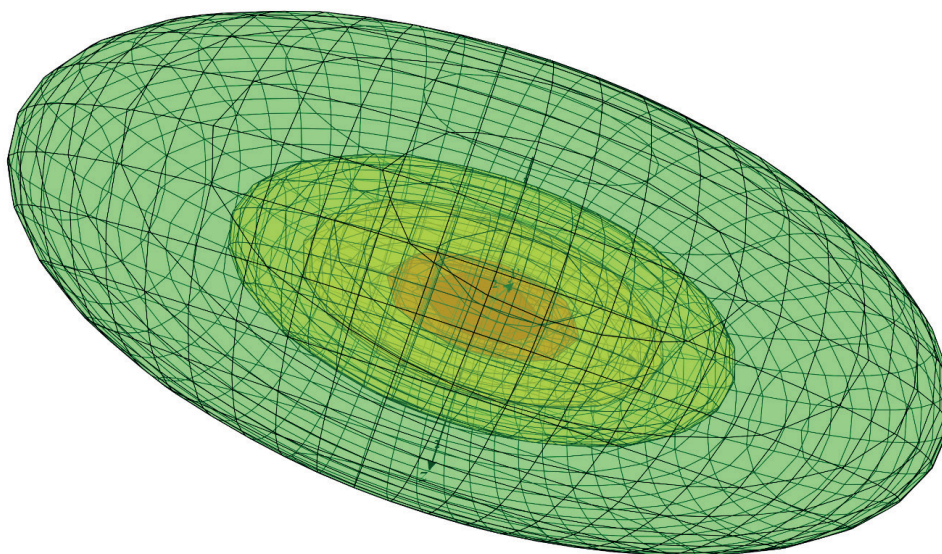


FIGURE 4: Graphical representation of layers of an ellipsoid ("probability density egg"), created with CalcPlot3D.

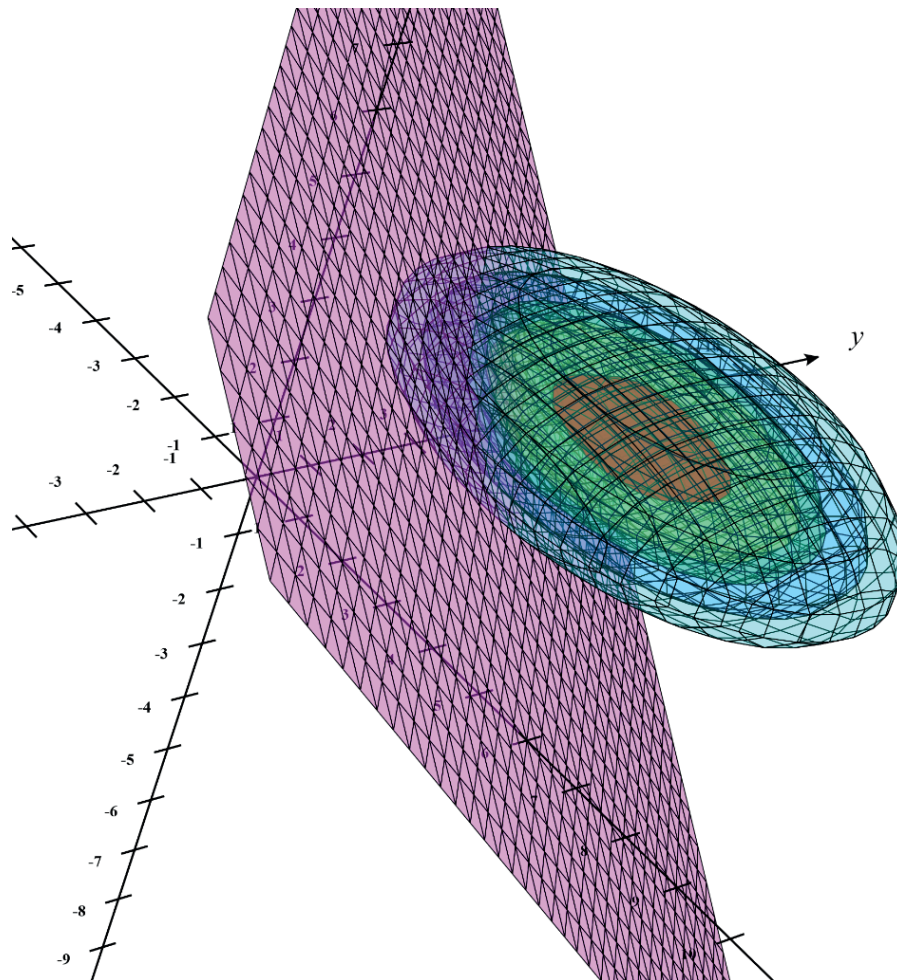


FIGURE 5: Linear data reconciliation.

disk lies in one plane (Figure 6 purple plane). On the intersection area (the plane with the probability density egg) one now looks for that point with the highest probability density. From here you look at the surface of the sphere again and see it again as a new disk lying at a new level. These steps are repeated until you have reached the last level. This plane differs from the others in that its point with the highest probability density exactly touches the sphere surface (manifold). This means that these coordinates (adjusted values) satisfy both the non-linear constraint and the local case of it (the last plane = tangent plane from the manifold) (Note that all other planes before that are not tangent planes of the manifold).

2.3.5 Determination of input parameters for aBM (C_{Cr} , C_{HF} , C_{Of} , C_{NF} , C_{Sf} and C_{Cb} , C_{Hb} , C_{Ob} , C_{Nb} , C_{Sb})

The elemental composition of water- and ash-free biogenic and fossil matter are input parameters which need to be defined when applying the aBM (to find the mathematical solution, the variances of the input values are also necessary). In this study, this was done based on extensive analyses (alternatively, literature values or data already collected could also be used; see. e.g. Schwarzboeck et.al., 2018b). The sorted nine fractions were cleaned from oil

and were analysed (elemental composition in the cleaned fraction and in the ash). Then, for each fraction a respective biogenic share was defined (estimation based on the aBM using literature values and on SDM results). And for each fraction an elemental composition of the biogenic and fossil share was defined. For example, for textiles a biogenic share of 70 to 80 wt% (water- and ash-free) was estimated based on pre-evaluations by means of the aBM and on SDM analyses. It was assumed that the elemental composition results from cellulose and wool in natural/biogenic textiles whereas in synthetic/fossil textiles different polymers are present (polyamid, polyester, polyacrylonitrile, polypropylene) (see also Schwarzboeck et al., 2018a and Kost, 2001). For "pure" fractions such as sorted plastics or paper, possible contamination by biomass (in plastic fraction) or by plastic (in paper fraction) was estimated (again by pre-evaluations by means of aBM and SDM). The elemental composition of these pure fractions was defined by own analyses of these fractions (which were corrected if contaminations were detected).

Finally, the elemental composition (C_{Cr} , C_{HF} , C_{Of} , C_{NF} , C_{Sf} and C_{Cb} , C_{Hb} , C_{Ob} , C_{Nb} , C_{Sb}) was derived by considering the mass shares per sorted fraction.

3. RESULTS AND DISCUSSION

3.1 Elemental composition of the material fractions (biogenic, fossil, oil) – used for aBM

The basis for defining the elemental composition in the material fractions were the sorted fractions (see Section 2.3.5 for details on the procedure). The result of the sorting is presented in Figure 7. It can be seen that the biogenic fraction is dominated by paper/cardboard (with 8.3 wt% in the RDF) and small amounts of wood (with 2 wt%). Further,

shares of the textile fraction, the composite fraction and the sorting residues contribute to the biomass (with biogenic shares estimated at 70 to 80 wt% in textiles and 60 to 70 wt% in composite and 65 to 90 wt% in sorting residues). The fossil fraction is defined by plastics (with sorted pure plastics comprising 17,7wt% in the RDF) and the counter shares in the mixed fractions mentioned.

The elemental values determined for the three material fractions are presented in Table 1. The values for biogenic and fossil matter are close to previously determined values

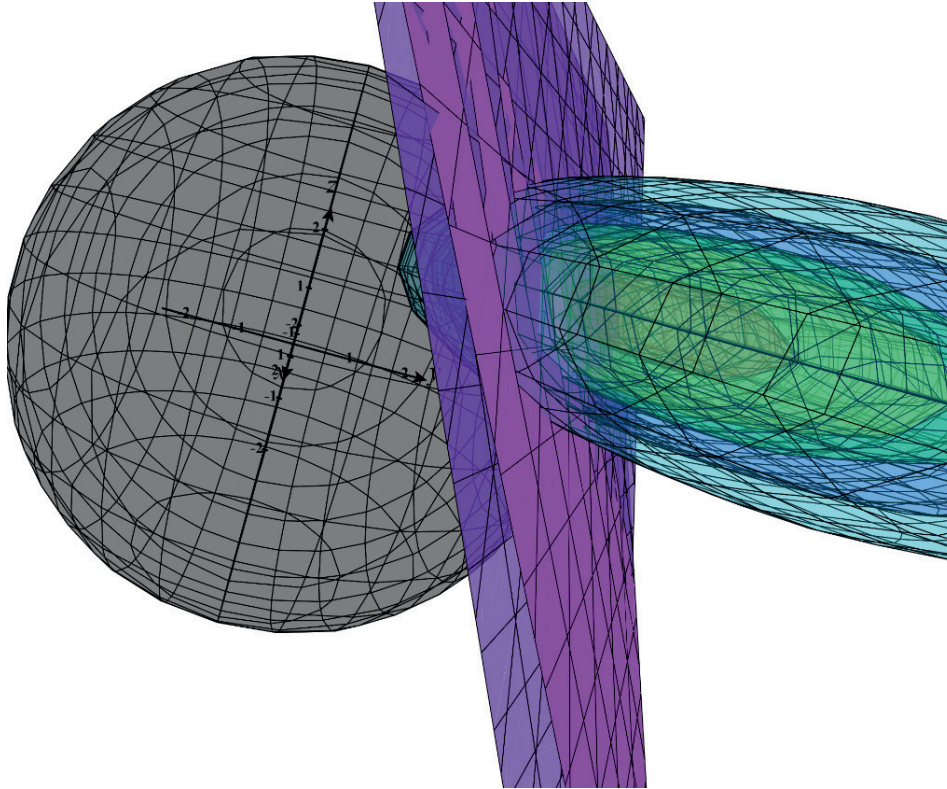


FIGURE 6: Non-linear data reconciliation.

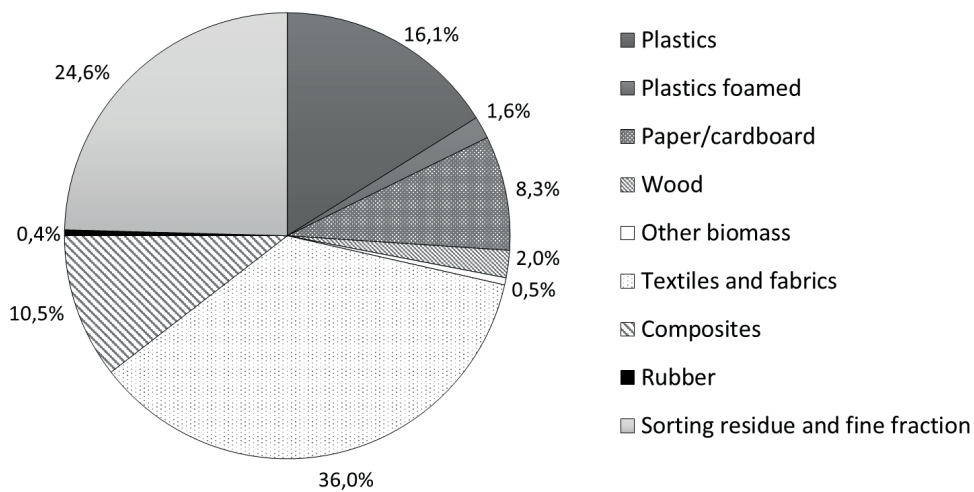


FIGURE 7: Fractional composition of the RDF (in wt%). The figures presented do not take the oil content in each fraction into consideration (each fraction has a different share of oil). Note that minor amounts of mineral materials (1.8wt%) and metals (0.2wt%) were additionally found but are not relevant for the evaluations presented.

TABLE 1: Determined elemental composition for biogenic and fossil matter and of the extracted oil from the RDF samples (results of one composite sample are presented).

	C _C	C _H	C _O	C _S	C _N
	g/kg _{waf}	g/kg _{waf}	g/kg _{waf}	g/kg _{waf}	g/kg _{waf}
Biogenic matter	467 ± 5	63.1 ± 2.0	474 ± 5	4.9 ± 1.0	12.2 ± 1.0
Fossil matter (without oil)	781 ± 7	113 ± 3	101 ± 3	4.6 ± 1.0	16.6 ± 1.2
Waste oil (fossil, extracted)	773 ± 3	131 ± 2	71.2 ± 5.9	9.3 ± 1.0	8.0 ± 1.0
Fossil matter (with oil)	780 ± 7	116 ± 3	96.5 ± 3.0	5.4 ± 1.0	15.1 ± 1.5

waf water-and ash-free

TABLE 2: Determined elemental composition of the RDF (results of one composite sample are presented).

	C _C	C _H	C _O	C _S	C _N
	g/kg _{waf}	g/kg _{waf}	g/kg _{waf}	g/kg _{waf}	g/kg _{waf}
RDF with oil-contamination	657 ± 14	87.0 ± 3.4	247 ± 8	7.8 ± 1.0	13.4 ± 1.0
RDF cleaned from oil-contamination	629 ± 18	86.8 ± 2.6	324 ± 17	6.9 ± 1.1	12.7 ± 1.0

waf water-and ash-free

for different RDFs (Schwarzboeck et al, 2018b). The elemental composition of oil is slightly below literature values found for waste oil or petroleum residues (e.g. in Phyllis database <https://phyllis.nl/> or UBA, 2016).

It can be seen that the carbon content in the fossil matter is very close to that determined in the extracted oil. Thus, this parameter cannot be used to distinguish between plastics ("fossil") and oil in this case. However, hydrogen content, oxygen content or sulphur content are more decisive in distinguishing between plastics ("fossil") and oil.

3.2 Shares of biomass, fossil matter and oil in RDF

Prior to calculating the mass shares in the RDF by applying the procedure described in the methods section in detail, the elemental composition of the RDF was analysed. The results of this analysis are summarized in Table 2.

Figure 8 shows the results for the mass shares (fossil, biogenic) determined without considering the oil contami-

nation. It can be seen that the method of selective dissolution (SDM) finds a similar fossil share in the RDF compared to the aBM (45.6 ± 2 wt% and 44.9 ± 3 wt%, respectively) (note that the results are given on a water- and ash-free basis).

The data reconciliation of the aBM adapted to three mass fractions was applied and the results are shown in Figure 9 (left side). The fossil share is estimated to be higher compared to the result in Figure 8. Additionally, the uncertainties of the results are rather high when applying the three-fractional data evaluation. Thus, the distinction between the mass shares is not as clear as in Figure 8. This is due to the rather close input values (elemental composition) of the fossil material fraction and of the oil (see Table 1). However, a plausible share of oil-contamination (around 14 wt%) was determined. The total fossil share was estimated at 56.9 ± 3.3 wt% and 57.5 ± 3.3 wt%, applying the three-fractional and two-fractional aBM-evaluation, respec-

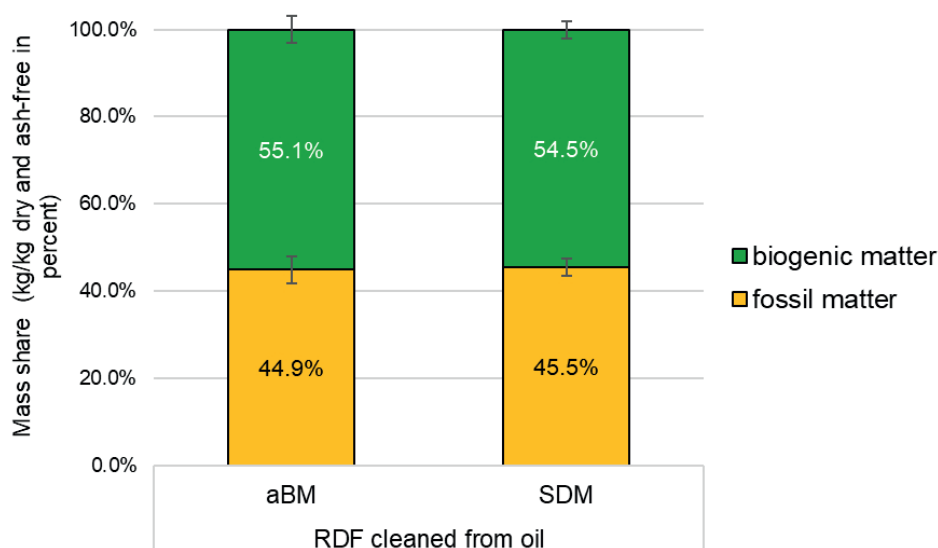


FIGURE 8: Mass shares as determined for RDF, which was cleaned from oil by balance equations (aBM) and by the chemical dissolution (SDM).

tively (Figure 9). Thus, these two evaluations result in values which are in a very close range. Comparing the results on the left side of Figure 9 (results of three-fractional evaluation) to the results on the right side of Figure 9 (results of two-fractional evaluation when the oil contamination is considered together with the fossil fraction), it can be seen that the uncertainty (variance) of the fossil mass fraction is reduced (by around one third) when only two mass fractions are determined. These differences in variances are again the result of the used input values being in a close range for fossil matter and for oil (also fossil). Additionally, covariances have not been considered so far, which could reduce the variances in the balanced data.

4. CONCLUSIONS

Evaluating waste-to-energy processes in terms of CO₂ mitigation requires appropriate methods to determine the relevant share of CO₂ in the feedstock (e.g. the share of plastics in the waste or in the RDF). In the study presented, for the first time the adapted Balance Method (aBM) was applied to RDF from hazardous waste (oil-contaminated). The aBM was adapted so that the method could be applied to determine three different fractions in RDF (biogenic, fossil, oil), instead of only two fractions. This is a novelty and was done by determining the elemental composition in the RDF (C, H, N, S, O) and by setting up balance equations containing the variables for the mass shares of biogenic, fossil and oil.

It was shown that the theory of the balance method in the higher dimensional space (26 dimensions) is based on mathematics that goes far beyond common mathematical knowledge. But in the low-dimensional 3-dimensional space it is possible to explain the solution to the problem graphically.

In general, the possibility of graphically describing the 3-dimensional normal distribution "probability density egg" should be made more widely known. Although this rep-

resentation is nothing new, as can be seen from the references, it is still not commonly used and is limited to the representation of 2-dimensional normal distribution.

Adapting the set of equations associated with aBM is a relatively easy undertaking. For this reason, adding even more variables (fractions) to be determined (e.g. certain types of plastics) is worth considering. This requires that the elemental composition be different from the other fractions in terms of at least two of the parameters (e.g. H and O). Further, a precondition for solving the equations is that there not be more variables than equations. Thus, the aBM is capable of distinguishing between more than two material fractions in RDF, which for other methods (such as selective dissolution or radiocarbon method) is not possible. The authors suggest intensified development efforts to increase the accuracy and to reduce the uncertainties of aBM. This could e.g. be done by determining and considering covariances in the mathematical algorithm or by introducing additional balance equations (e.g. for ash content). A further current limitation of the aBM is that the elemental composition needs to be defined beforehand for the sought-after fractions, which can be labor intensive and can limit applicability. Thus, more data need to be collected based on a broader variety of samples and the use of literature values needs to be further investigated. One step to ease the application of aBM has been taken by the authors by initiating development of a versatile software application for aBM evaluation. Some data have already been collected in Schwarzboeck et al. (2018b).

The aBM can in future support the characterization of RDFs and the carbon footprint evaluation of waste-to-energy processes. Reliable and cost-efficient characterization methods are particularly relevant in producing industries where RDFs are utilized as substitute for fossil fuels (relevant for both the producer and the user of RDFs). With aBM being able to differentiate also between more material fractions, the method could also become a viable tool in the context of recycling and material recovery (e.g. determin-

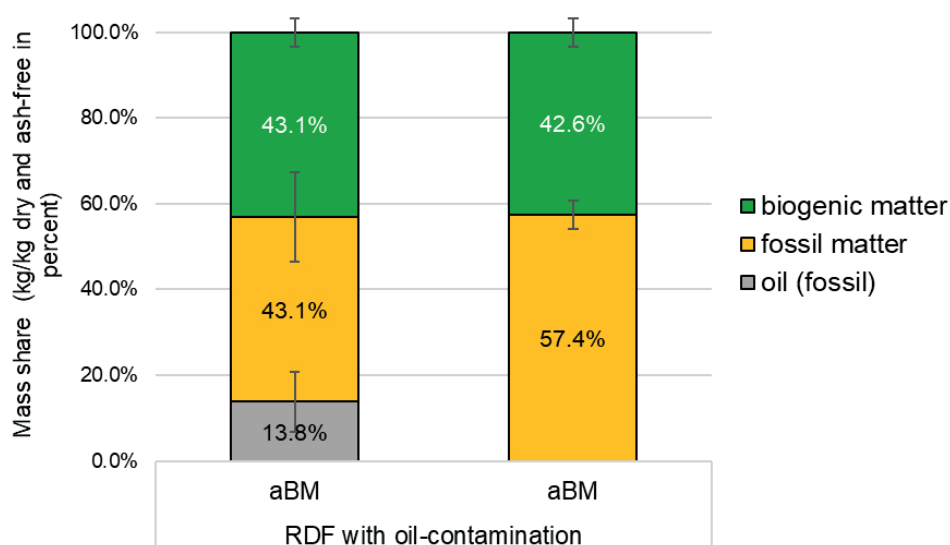


FIGURE 8: Mass shares as determined for RDF, which was cleaned from oil by balance equations (aBM) and by the chemical dissolution (SDM).

ing the share of unwanted or wanted plastics in RDFs or at the input of recycling facilities).

ACKNOWLEDGEMENTS

The authors would like to thank the RDF plant operator for drawing the samples and for their support.

REFERENCES

- Anderl, M., Colson, J., Gangl M., Kuschel, V., Mandl, N., Matthews, B., Mayer, M., Mayer, S., Moldaschl, E., Pazdernik, K., Poupá, S., Purzner, M., Rockenschaub, A.K., Roll, M., Schieder, W., Schmidt, G., Schodl, B., Schwaiger, E., Schwarzl, B., Stranner, G., Weiss, P., 2023. Austria's Annual Greenhouse Gas Inventory 1990-2021. Submission under Regulation (EU) No 2018/1999. Report REP-0841, <https://www.umweltbundesamt.at/>.
- Aranda Usón, A., López-Sabirón, A.M., Ferreira, G., Llera Sastresa, E., 2013. Uses of alternative fuels and raw materials in the cement industry as sustainable waste management options. *Renewable and Sustainable Energy Reviews* 23, 242-260. <https://doi.org/10.1016/j.rser.2013.02.024>.
- EN ISO 21640: Solid recovered fuels – Specifications and classes. German version EN ISO 21640:2021. DIN-Normenausschuss Materialprüfung (NMP).
- EN ISO 21644: Solid recovered fuels – Methods for the determination of biomass content. German version EN ISO 21644:2021. DIN-Normenausschuss Materialprüfung (NMP).
- European Parliament: Directive 2009/29/EC on amending Directive 2003/87/EC so as to improve and extend the greenhouse gas emission allowance trading scheme of the Community. *Official Journal of the European Union*, pp. 63–87.
- Fellner J., Rechberger H. 2009. Abundance of ¹⁴C in biomass fractions of wastes and solid recovered fuels, *Waste Management*, Volume 29, Issue 5, 2009, Pages 1495-1503, <https://doi.org/10.1016/j.wasman.2008.11.023>.
- Fellner J, Aschenbrenner P, Cencic O, Rechberger H. Determination of the biogenic and fossil organic matter content of refuse-derived fuels based on elementary analyses. *Fuel* 2011;90(11):3164–71. <http://dx.doi.org/10.1016/j.fuel.2011.06.043>.
- Gałko, G., Mazur I., Rejdak M., Jagustyn B., Hrabak, J., Ouadi, M., Jahangiri, H., Sajdak, M., 2023. Evaluation of alternative refuse-derived fuel use as a valuable resource in various valorised applications, *Energy*, Volume 263, Part D, 2023, 125920, <https://doi.org/10.1016/j.energy.2022.125920>.
- Garg A., Smith, R., Hill, D., Simms, N., Pollard, S. 2007. Wastes as Co-Fuels: The Policy Framework for Solid Recovered Fuel (SRF) in Europe, with UK Implications, *Environmental Science & Technology* 2007 41 (14), 4868-4874, <https://doi.org/10.1021/es062163e>.
- Genon, G., Brizio, E. 2008, Perspectives and limits for cement kilns as a destination for RDF, *Waste Management*, Volume 28, Issue 11, 2008, Pages 2375-2385, <https://doi.org/10.1016/j.wasman.2007.10.022>.
- Habert, G., Billard, G., Rossi, P., Chen, C., Roussel, N. 2010. Cement production technology improvement compared to factor 4 objectives, *Cement and Concrete Research*, Volume 40, Issue 5, 2010, Pages 820-826, <https://doi.org/10.1016/j.cemconres.2009.09.031>.
- Hiroimi Ariyaratne, W.H., Melaaen, M.C., Tokheim, L.A., Determination of biomass fraction for partly renewable solid fuels 2014, *Energy*, 70, 465 – 472. <https://doi.org/10.1016/j.energy.2014.04.017>.
- Ke, T., Lv, H., Sun, M., Zhang, L. A bisected least squares support vector machine based on Mahalanobis distance for PU learning. *Physica A* (2018), 422-438. <https://doi.org/10.1016/j.physa.2018.05.128>.
- Kost T., Brennstofftechnische Charakterisierung von Haushaltsabfällen (in German: Fuel Characterization of Household Waste) (Ph.D.Thesis), Dresden Technical. University, Dresden, Germany, 2001.
- Larsen, A.W.; Fuglsang, K.; Pedersen, N.H., Fellner, J.; Rechberger, H.; As-trup, T.:2013. Biogenic carbon in combustible waste: Waste composition, variability and measurement uncertainty. *Waste Manage Res* 31, 2013, pp. 56-66. <https://doi.org/10.1177/0734242X13502387>.
- Moorá H., Roos I., Kask, U., Kask, L., Ounapuu, K., Determination of biomass content in combusted municipal waste and associated CO₂ emissions in Estonia 2017, *Energy Procedia*, 128, 222 – 229. <https://doi.org/10.1016/j.egypro.2017.09.059>.
- Muir, G.K., Hayward, S., Tripney, B.G., Cook, G.T., Naysmith, P., Herbert, B.M., Garnett, M.H., Wilkinson, M., 2015. Determining the biomass fraction of mixed waste fuels: a comparison of existing industry and (14)C-based methodologies. *Waste Manage.* 35, 293–300. <https://doi.org/10.1016/j.wasman.2014.09.023>.
- Nasrullah M, Vainikka P, Hannula J, Hurme M, Karki J. Mass, energy and material balances of SRF production process. Part 1: SRF produced from commercial and industrial waste. *Waste Manage* 2014;34(8):1398–407. <http://dx.doi.org/10.1016/j.wasman.2014.03.011>.
- Rada, E.C, Ragazzi, M. 2014. Selective collection as a pretreatment for indirect solid recovered fuel generation, *Waste Management*, Volume 34, Issue 2, 2014, Pages 291-297, <https://doi.org/10.1016/j.wasman.2013.11.013>.
- Rueda, L. G., Oommen, B. J. On optimal pairwise linear classifiers for normal distribution: the d-dimensional case. *Pattern Recognition* 36 (2003), 13-23. [https://doi.org/10.1016/S0031-3203\(02\)00053-5](https://doi.org/10.1016/S0031-3203(02)00053-5).
- Sarc, R., Lorber, K., Pomberger, R., Rogetzer, M., Sippl, E., 2014. Design, quality, and quality assurance of solid recovered fuels for the substitution of fossil feedstock in the cement industry. *Waste Manage Res* 32, 565-585. <https://doi.org/10.1177/0734242X14536462>.
- Schwarzböck, T., Aschenbrenner, P., Spacek, S., Szidat, S., Rechberger, H. and Fellner, J., 2018a. An alternative method to determine the share of fossil carbon in solid refuse-derived fuels – Validation and comparison with three standardized methods. *Fuel* 220, 916-930. <https://doi.org/10.1016/j.fuel.2017.12.076>.
- Schwarzböck, T., Aschenbrenner, P., Muehlbacher, S., Szidat, S., Spacek, S. and Fellner, J., 2018b. Determination of the climate relevance of refuse derived fuels - validity of literature-derived values in comparison to analysis-derived values. *Detritus* 2, 120-132. <https://doi.org/10.31025/2611-4135/2018.13649>.
- Schwarzböck, T., 2018. Determination of biogenic and fossil matter in wastes, refuse-derived fuels and other plastic-containing mixtures - Potentials and limitations. Doctoral Thesis. Supervisor: Johann Fellner; Institute for Water Quality and Resource Management, Technische Universität Wien (TU Wien). 2018. <https://doi.org/10.34726/hss.2018.59301>.
- UBA, 2016. Umweltbundesamt (environmental protection agency Germany). CO₂-Emissionsfaktoren für fossile Brennstoffe. *CLIMATE CHANGE* 27/2016. Kristina Juhlich, Fachgebiet Emissionssituation, ISSN 1862-4359. <https://www.umweltbundesamt.de/publikationen>.
- Viczek, S.A., Aldrian, A., Pomberger, R., Sarc, R., 2020. Origins and carriers of Sb, As, Cd, Cl, Cr, Co, Pb, Hg, and Ni in mixed solid waste – A literature-based evaluation, *Waste Management*, Volume 103, 2020, Pages 87-112, <https://doi.org/10.1016/j.wasman.2019.12.009>.
- Wu, S., Ye, Q., Chen, C., Gu, X., 2015. Research on data reconciliation based on generalized T distribution with historical data. *Neuro-computing* 175 (2016), 808-815. <https://doi.org/10.1016/j.neucom.2015.10.093>.